*Available online at* www.scholarsresearchlibrary.com

Scholars Research Library

**Der Pharmacia Lettre, 2018, 10 [7]: 33-47**
*[http://scholarsresearchlibrary.com/archive.html]*

ISSN 0975-5071
USA CODEN: DPLEB4

# Molecular Docking Studies of Substituted Benzopyan-2-one Derivatives as α-Glucosidase Inhibitors and ADMET Analysis

**Samridhi Thakral and Vikramjeet Singh***

*Department of Pharmaceutical Sciences, Guru Jambheshwar University of Science and Technology, Hisar, Haryana*

****Corresponding author:** Singh V, Assistant Professor, Department of Pharmaceutical Sciences, Guru Jambheshwar University of Science and Technology, Hisar, India, Tel: +919416595369 E-mail: vikramjeetsinghjudge@gmail.com*

---

**ABSTRACT**

*Diabetes mellitus is a ubiquitous challenge and accounts for 387 million patients globally and this figure will ascent to over 590 million by the year 2035. α-Glucosidase inhibitors results in decrease in postprandial blood glucose level by delaying of glucose absorption. Two series of substituted benzopyran-2-one derivatives were appraised by molecular docking studies, drug-likeness and ADMET properties predictions. Compounds 8, 10, 19, 21 exhibited strong binding interactions such as hydrogen bonding, hydrophobic and electrostatic interactions with 3D α-glucosidase modeled protein because of presence of OH group at $R^2$ position. Top most active compound 21 (7-hydroxy-6-methoxy-3-[4-(4-methyl-phenylsulfonamido)benzoyl]-2H-1-benzopyran-2-one) interacted with protein by forming 3 hydrogen bonding and pi-pi stacked, pi-pi T shaped, pi-alkyl and pi-anion interactions. The consequences of in silico pharmacokinetic inferred their potential as potent α-glucosidase inhibitor.*

**Keywords:** Enzyme inhibitors, Homology modeling, Ligand, Molecular docking, *In silico* ADMET screening.

---

## INTRODUCTION

Diabetes mellitus is an endocrine disorder which is associated with various complications such as retinopathy, neuropathy, nephropathy, cardiovascular diseases [1,2]. Postprandial hyperglycemia is a feature of DM, which is generally characterized by an abnormal rise in blood sugar right after a meal. Therefore, to combat this disorder, one of the numerous approaches is to develop enzymes inhibitors that are responsible for hydrolyzing amylopectin, starch and the carbohydrates to glucose [3]. As a consequence, α-glucosidase is a crucial target for type II diabetes treatment and their inhibitors binds to α-glucosidase and delay the carbohydrates absorption from the small intestine, thus helps in lowering the blood glucose level [4].

The pharmaceutical industry has progressively implemented modern medicinal chemistry methods, inclusive of molecular modeling, as impressive tool for the appraisal of structure-activity relationships (SAR) [5]. In field of molecular modeling, molecular docking which is structure-based drug design, an ordinarily method which predicts the preferred confirmations of ligands as small molecules to binding site of target protein [6]. In various stages of drug design strategies, docking is frequently used for assistance in design of potentially active leads [7]. Two basic steps are involved in docking process such as computation of the ligands conformation along with its orientation and position within these sites, referred as pose and evaluation of the binding affinity of ligands molecules with target proteins [8]. In continuation of our efforts towards computational studies of active molecules [9-11] in this present study we have screened α-glucosidase inhibitors reported by Wang et al. [12] for antidiabetic potential by *in silico* approach including molecular docking and ADMET analysis.

## MATERIALS AND METHODS

### *Preparation of ligand molecules*

A recent study by Wang et al. on α-glucosidase inhibitors, 22 derivatives synthesized by them were screened through *in vitro* evaluation [12]. We have considered all 22 derivatives as ligands molecule for our present study to understand the binding interactions with α-glucosidase enzymes. The 2D structures of reported molecules were sketched in MarvinSketch and saved in pdb format, which were later converted into pdbqt format by using AutoDock tools.

### *Homology modeling*

The crystallographic structure for intestinal α-glucosidase enzyme is not accessible up to yet. So this compensation is done by developing 3D model of α-glucosidase by comparative homology Based on previous works and existing knowledge [13], 3D

structure was modeled by SWISS-MODEL web server (https://swissmodel.expasy.org/) [14] using crystallographic structure of *Saccharomyces cerevisiae* isomaltase (PDB code 3AJ7) [15] as a template because it showed 72.4% sequence identity with our query sequence which (P53341) was retrieved from UniProt (http://www.uniprot.org/). The output structure obtained from SWISS-MODEL server, which was then kept in the centre of the cubic box, the rest of the volume of box was filled by SPCe [16] water molecules. The 16 $Na^+$ ions were added in entire box to neutralize the 16 e- charge in place of the respective number of water molecules. Thereafter energy minimization was done and then 10 ns equilibration carried out by using OPLS [17] force fields integrated into GROMACS 5.4 [18] package to depict the potential energy of the system. Ramachandran plot was used for validation of quality of model by RAMPAGE (http://mordred.bioc.cam.ac.uk/~rapper/rampage.php).

***Preparation of protein***

Molecular docking studies were rendered by using advanced docking program AutoDock Vina to evaluate the binding interactions of reported compounds into the active sites of 3D modeled structure of α-glucosidase enzyme. Polar hydrogen atoms were appended and removed the water molecules which did not participate in interactions and then modeled protein was saved in PDBQT format. The docking studies were carried out in accordance with specified conditions of grid box auto generated by AutoDock tools [19]. The Vina search space chosen was center_x= 47.316, center_y= 59.029, center_z= 55.525 for developed protein of α–glucosidase with dimension size_x= 40, size_y= 40, size_z= 40. The exhaustiveness was set to be 8. The results were visualized using PyMol and Discovery studio visualizer [20].

***Pharmacokinetic properties prediction***

Molinspiration (http://www.molinspiration.com/) online tool kit and OSIRIS property explorer were used for evaluating the drug-like properties by computing a set of parameters of 2D chemical structures [21]. Pre-ADMET online server (https://preadmet.bmdrc.kr/) was used for prediction of the pharmacokinetics parameters like absorption, distribution, metabolism, excretion, and toxicity of reported compounds [22]. OSIRIS property explorer also helped in the prediction of various toxicity parameters like mutagenicity, tumorigenicity, irritating effects, and reproductive effects [23].

## RESULTS AND DISCUSSION

***Molecular docking***

Molecular dynamic simulation of modeled structure was carried out by GROMACS 5.4 for 10 ns. The RMSD map analysis (Figure 1) of backbone atoms throughout MD simulation signifying that in last 5 ns trajectory of equilibration run the structure is reaching to a stable state. The superimposed structure of final protein obtained after homology modeling on the template

isomaltase from *Saccharomyces cerevisiae* (PDB: 3AJ7) is represented by Figure 2. Both proteins possess similar folding structure to a certain extent as inferred from the superimposition. The evaluation of Ramachandran plot which displays graphical representation of Phi, Psi (torsion) angles distributions for all residues indicated that most of the amino acid residues were in favored region with a percentage of 90% while 9.3% of residues in allowed region and 0.7% residues in outlier region (Figure 3).

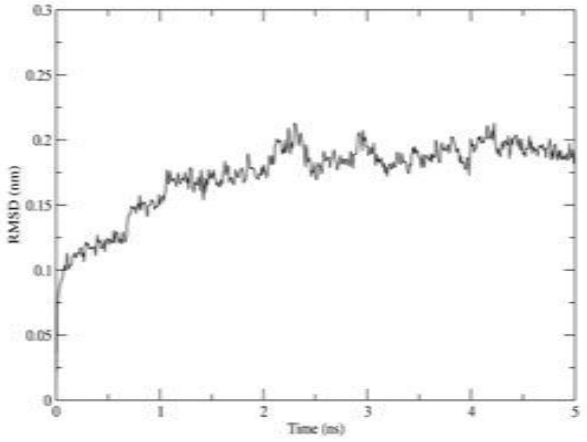


**Figure 1:** RMSD plot of protein backbone atoms vs. time of last 5 ns trajectory of equilibration run.

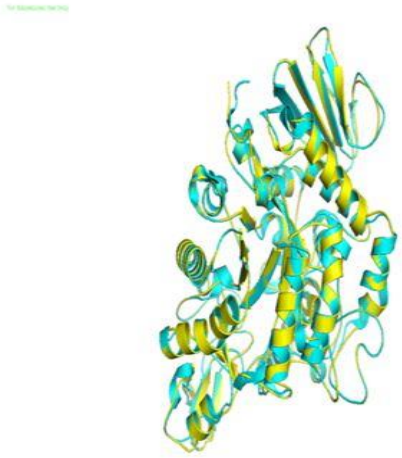

**Figure 2**: The superimposed structure of the modeled α-glucosidase (yellow) on the template oligo-1,6-glucosidase (Cyan) obtained from isomaltase from *Saccharomyces cerevisiae.*

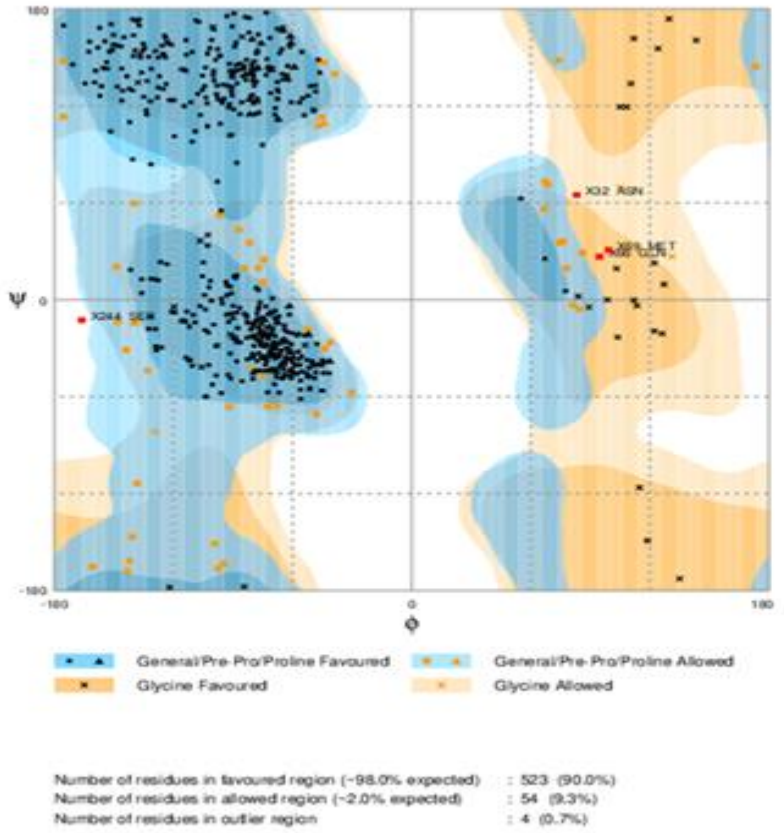


**Figure 3:** Ramachandran plot of homology modeled 3D structure.

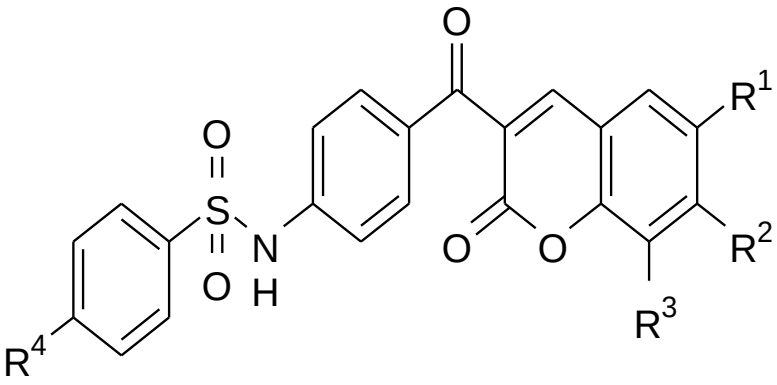


**Figure 4:** General structure of reported compounds.

**Table 1:** Structure of compounds and their binding energy.

| Comp. | $R^1$ | $R^2$ | $R^3$ | $R^4$ | Binding Energy (Kcal/mol) | Comp. | $R^1$ | $R^2$ | $R^3$ | $R^4$ | Binding Energy (Kcal/mol) |
|---|---|---|---|---|---|---|---|---|---|---|---|
| 1 | H | H | H | H | -10.3 | 12 | H | H | H | $CH_3$ | -10.6 |
| 2 | F | H | H | H | -10.6 | 13 | F | H | H | $CH_3$ | -10.7 |
| 3 | Cl | H | H | H | -10.2 | 14 | Cl | H | H | $CH_3$ | -10.4 |
| 4 | Br | H | H | H | -9.9 | 15 | Br | H | H | $CH_3$ | -10.3 |
| 5 | Br | H | Br | H | -9.8 | 16 | Br | H | Br | $CH_3$ | -10.3 |
| 6 | $C(CH_3)_3$ | H | $C(CH_3)_3$ | H | -10.3 | 17 | $C(CH_3)_3$ | H | $C(CH_3)_3$ | $CH_3$ | -10.5 |
| 7 | H | $OCH_3$ | H | H | -9.8 | 18 | H | $OCH_3$ | H | $CH_3$ | -9.8 |
| 8 | H | OH | H | H | -9.8 | 19 | H | OH | H | $CH_3$ | -10.7 |
| 9 | H | $N(C_2H_5)_2$ | H | H | -9.2 | 20 | H | $N(C_2H_5)_2$ | H | $CH_3$ | -9.8 |
| 10 | $OCH_3$ | OH | H | H | -9.6 | 21 | $OCH_3$ | OH | H | $CH_3$ | -10.2 |
| 11 | $OCH_3$ | $OCH_3$ | H | H | -9.8 | 22 | $OCH_3$ | $OCH_3$ | H | $CH_3$ | -10.3 |

The compounds selected for study can be broadly divided in to two series (Table 1), one unsubstituted ($R^4$=H)/phenyl sulfonamide derivatives and another is methylated derivatives ($R^4$=$CH_3$,)/4-methyl phenyl sulfonamide derivatives. In both series, compounds **8** ($R^2$-OH), **10** ($R^1$-$OCH_3$, $R^2$-OH) and **19** ($R^2$-OH), **21** ($R^1$-$OCH_3$, $R^2$-OH) exhibited three hydrogen bonding interactions as compared to all derivatives and showed more inhibitory potential against α-glucosidase enzyme.

In the first series where $R^4$=H, a potential binding interaction was found between compound 10 with modeled protein (Figure 4). The molecular docking study revealed that this molecule in modeled protein exhibit hydrogen bonding, hydrophobic and electrostatic interactions with active site residues. The OH group created a hydrogen bond interaction with carbonyl oxygen of Phe: 157 at a distance of 2.11 Å. Both C=O of benzopyran-2-one established one hydrogen bond with NH of Arg: 439 having bond length of 2.60 Å. This compound was also able to form one hydrogen bond with Glu: 276 using the NH of $SO^2NH$ (2.22 Å). The binding of this molecule also facilitated hydrophobic and electrostatic interactions. The phenylsulfonamido ring were mainly engaged in hydrophobic interactions with His: 348, Tyr: 344, Phe: 298 (5.29 Å, 5.06 Å, 4.10 Å) by forming pi-pi T shaped and pi-pi stacking interactions. Benzopyran-2-one ring also formed pi-pi T shaped with Phe: 177 with bond length of 5.90 Å. The electrostatic interactions (pi-anion) were also observed by Asp: 349, Asp: 214 amino acid residues. Compound 8 formed similar types of interaction with modeled protein.

In the methylated series where $R^4$=$CH_3$, considering the top ranked most potent compound 21 bearing $R^4$=$CH_3$, displayed similar three hydrogen bonding, hydrophobic and electrostatic interactions while some additional hydrophobic binding interactions were observed as compared to compound 10 (Figure 5). Tyr: 344, Phe: 298, Trp: 57, His: 348 showed pi-alkyl interactions with $CH_3$ group at a distance of 4.36 Å, 4.61 Å, 5.12 Å and 4.93 Å respectively. Compound 19 formed similar types of interaction with modeled protein.

Three hydrogen bond formations were observed in compound 8 ($R^2$-OH) in comparison to 7 ($R^2$-$OCH_3$, one hydrogen bond). This result implied that the presence of hydrogen bonding interactions may be contributing to better activity of compound 8. Comparison of 19 ($R^2$-OH) with 18 ($R^2$-$OCH_3$), 19 formed three hydrogen bonding interactions whereas in compound 18 two hydrogen bond interactions were observed. Compound 19 also formed 2 additional pi-anion interactions with Asp: 349 with bond lengths of 3.87 Å and 4.12 Å respectively. This resulted in increase in inhibitory activity of 19.

The comparison of compounds 10 ($R^1$-$OCH_3$, $R^2$-OH) and 21 ($R^1$-$OCH_3$, $R^2$-OH) with compounds 11 ($R^1$-$OCH_3$, $R^2$-$OCH_3$) and 22 ($R^1$-$OCH_3$, $R^2$-$OCH_3$), 10 and 21 exhibited three hydrogen bonding interactions while 11 and 22 displayed one hydrogen bond. This result inferred that the H-bonding interactions contributed to better activity of compounds

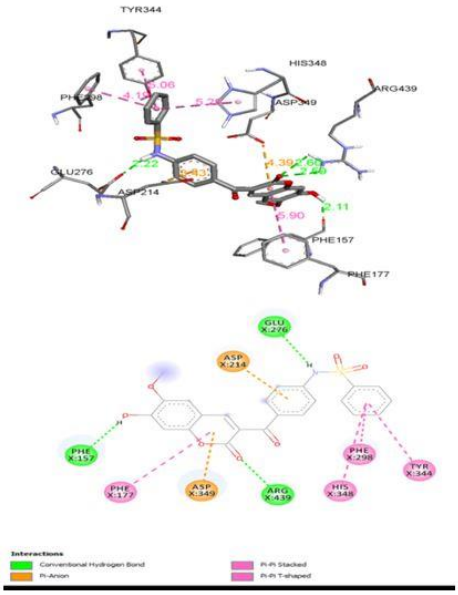


**Figure 5:** The 3D binding model of compound 10 into active site of 3D modeled structure and 2D model of binding pose of interacting amino acid residues of 3D modeled structure with docked compound 10 with bond lengths.

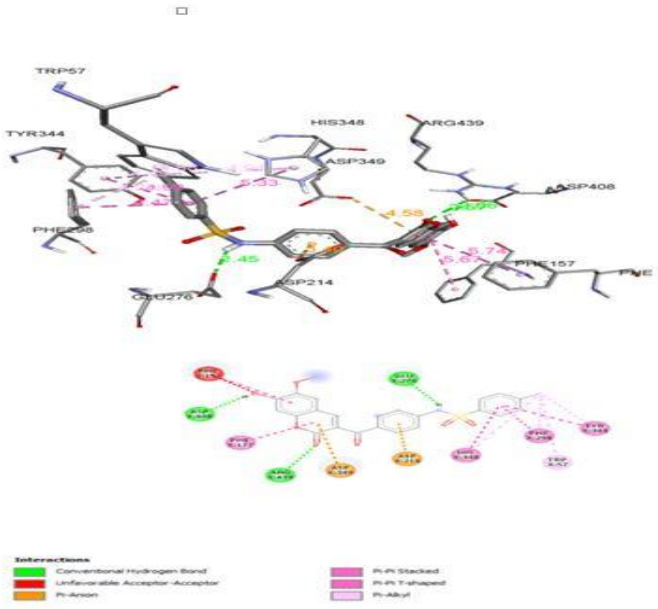


**Figure 6:** The 3D binding model of compound 21 into active site of 3D modeled structure and 2D model of binding pose of interacting amino acid residues of 3D modeled structure with docked compound 21 with bond lengths.

In case of first series where $R^4$=H, a decrease in inhibitory potential against α-glucosidase enzyme was observed as modification of benzopyran one moiety with halogens was done like in compounds 2 ($R^1$-F), 3 ($R^1$-Cl), 4 ($R^1$-Br), 5 ($R^1$-Br, $R^3$-Br), exhibited decrease in α-glucosidase inhibitory activity because only F allowed to form a halogen bond with the receptor. Similar types of results were observed in methylated series.

The results revealed that methylated series displayed more inhibitory potential against α-glucosidase enzyme as compared to unsubstituted phenyl sulfonamide series because in all compounds (12-22) $CH_3$ was found to engaged in forming pi-alkyl interactions with Tyr: 344, Phe: 298, Trp: 57, His: 348 amino acid residues. Some common hydrophobic interactions were also found with Phe: 298, His: 348, Tyr: 344, Tyr:71, Phe: 300, Phe: 177, Phe: 158 and electrostatic (pi-anion) interactions were observed with Glu: 276, Asp: 349, Asp: 214 amino acid residues.

**Prediction of drug relevant parameters**

According to Lipinski rule of five, descriptors of compounds like $\log_P$ values should be not higher than five, molecular weight not more than 500, number of hydrogen bond acceptor and hydrogen bond donors not more than 10 and 5, respectively. Polar

surface area and number of rotatable bonds also influence the oral bioavailability of drug molecules [24]. According to veber's rule, rotatable bonds should not more than 10 and polar surface area should not more than 140 Å2 [25]. The imperative pharmacokinetic parameters with their acceptable ranges are represented in Table 2. The reported benzopyranone derivatives were found to follow Lipinski rule of five and Weber's rule except some compounds 5, 6, 14, 15, 16, 17, 20 which showed maximum violations of 2 rules. Two violations of Lipinski rule of five are acceptable for an orally active molecule [26].

***In silico* ADMET Study**

Some of the computed properties are $CaCO_2$ cell permeability (nm/s), human intestinal absorption (HIA%), MDCK (Medin-Darbey Canine Kidney Epithelial Cells) cell permeability.

**Table 2:** Prediction of Lipinski rule of five and Veber's rule for substituted benzopyran-2 one derivatives using molinspiration online tool kit and OSIRIS property explorer.

| Comp. | Milog P[a] | Log S[b] (mol/L) | TPSA[c] (Å$^2$) | MW[d] | nON[e] | nOHNH[f] | nVoilations[g] | nRot[h] | Volume |
|---|---|---|---|---|---|---|---|---|---|
| 1 | 4.16 | -2.7903 | 93.45 | 405.43 | 6 | 1 | 0 | 5 | 334.22 |
| 2 | 3.33 | -5.457 | 93.45 | 423.42 | 6 | 1 | 0 | 5 | 339.15 |
| 3 | 4.82 | -5.879 | 93.45 | 439.88 | 6 | 1 | 0 | 5 | 347.76 |
| 4 | 4.95 | -5.977 | 93.45 | 484.33 | 6 | 1 | 0 | 5 | 352.11 |
| 5 | 5.68 | -6.811 | 93.45 | 563.22 | 6 | 1 | 2 | 5 | 369.99 |
| 6 | 7.48 | -7.463 | 93.45 | 517.65 | 6 | 1 | 2 | 7 | 466.59 |
| 7 | 4.20 | -5.161 | 102.69 | 435.46 | 7 | 1 | 0 | 6 | 359.77 |
| 8 | 3.66 | -4.847 | 113.68 | 421.43 | 7 | 2 | 0 | 5 | 342.24 |
| 9 | 4.99 | -5.779 | 96.69 | 476.25 | 7 | 1 | 0 | 8 | 413.73 |
| 10 | 3.48 | -4.865 | 122.91 | 451.46 | 8 | 2 | 0 | 6 | 367.79 |
| 11 | 3.79 | -5.179 | 111.92 | 465.48 | 8 | 1 | 0 | 7 | 385.31 |
| 12 | 4.61 | -5.487 | 93.45 | 419.46 | 6 | 1 | 0 | 5 | 350.78 |
| 13 | 3.78 | -5.801 | 93.45 | 437.45 | 6 | 1 | 0 | 5 | 355.71 |
| 14 | 5.26 | -6.223 | 93.45 | 453.90 | 6 | 1 | 1 | 5 | 364.32 |
| 15 | 5.40 | -6.321 | 93.45 | 498.35 | 6 | 1 | 1 | 5 | 368.67 |
| 16 | 6.13 | -7.155 | 93.45 | 577.25 | 6 | 1 | 2 | 5 | 386.55 |
| 17 | 7.93 | -7.807 | 93.45 | 531.67 | 6 | 1 | 2 | 7 | 483.15 |
| 18 | 4.64 | -5.505 | 102.69 | 449.48 | 7 | 1 | 0 | 6 | 376.33 |
| 19 | 4.11 | -5.191 | 113.68 | 435.46 | 7 | 2 | 0 | 5 | 358.80 |
| 20 | 5.44 | -6.123 | 96.69 | 490.58 | 7 | 1 | 1 | 8 | 430.29 |
| 21 | 3.93 | -5.209 | 122.91 | 465.48 | 8 | 2 | 0 | 6 | 384.35 |
| 22 | 4.23 | -5.523 | 111.92 | 479.51 | 8 | 1 | 0 | 7 | 401.87 |

[a]Logarithm of partition coefficient between n-octanol and water (miLog P); [b]Solublity (LogS); [c]Topological polar surface area

(TPSA); [d]Molecular weight (MW); [e]Number of hydrogen bond aceeptor (nON); [f]Number of hydrogen bond donor (nOHNH); [g]Number of violations (nvoilations); [h]Number of rotatable bonds (nrot). (nm/s), blood brain barrier penetration (C. brain/C. blood), plasma protein binding (%).

Pgp inhibition and results are tabulated in Table 3 [27]. The human intestinal absorption values vary from 94.961 to 97.556% which established the absorption capacity of reported compounds and endorsed their interaction with target cell. The *in vitro* $CaCO_2$ cell permeable property vary from 0.927-19.900 nm/s, *in vitro* MDCK cell permeability vary from 0.019-0.221 nm/s designated moderate and low permeability of reported compounds with the concerned cell line, respectively. The synthesized compounds displayed values in range of 90.933-97.741% confirmed their strong protein binding capacity. The *in vivo* blood brain barrier penetration vary from 0.015 to 0.392 supported their distribution *in vivo* with low to moderate penetration capacity. Table 4 represented toxicity risk of reported compounds obtained from OSIRIS property explorer.

The inclusion of various substituents in benzopyran-2-one derivatives leads to amendment of enzymatic activity and all these facts can be summarized as represented by Figures 6 and 7.

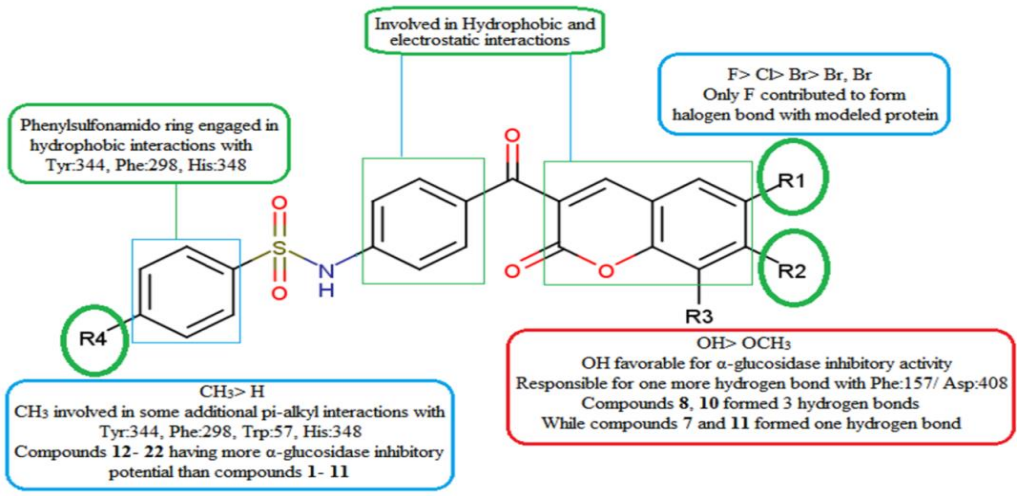


**Figure 7:** Essential features of benzopyran-2-one derivatives for α-glucosidase inhibitory activity.

**Table 3:** Evaluation of pharmacokinetic parameters of substituted benzopyran-2-one derivatives using Pre-ADMET online server.

| **Comp.** | **Human Intestinal absorption HIA (%)** | ***In vitro* $CaCO_2$ cell permeability (nm/s)** | ***In vitro* MDCK cell permeability (nm/s)** | ***In vivo* plasma protein binding (%)** | ***In vivo* blood brain barrier penetration (C. brain/C. blood)** | **PGP_ inhibition** |
|---|---|---|---|---|---|---|
| | Poor absorption-0-20% Moderate absorption-20- 70% Well absorption-70-100% | Low permeability-<4 Moderate permeability-4-70 High permeability->70 | Low permeability-<25 Moderate permeability-25-500 High permeability->500 | Weak binding-<90% Strong binding->90% | Low absorption-<0.1 Moderate absorption-0.1-2.0 Higher absorption->2.0 | |
| 1 | 96.396 | 08.084 | 0.151 | 94.752 | 0.015 | Inhibitor |
| 2 | 96.395 | 08.543 | 0.080 | 94.984 | 0.016 | Inhibitor |
| 3 | 96.539 | 03.278 | 0.065 | 94.159 | 0.019 | Inhibitor |
| 4 | 96.795 | 01.177 | 0.020 | 93.272 | 0.020 | Inhibitor |
| 5 | 97.482 | 02.125 | 0.022 | 94.598 | 0.034 | Inhibitor |
| 6 | 96.783 | 19.545 | 0.044 | 97.339 | 0.188 | Inhibitor |
| 7 | 96.731 | 11.960 | 0.168 | 93.959 | 0.019 | Inhibitor |
| 8 | 94.961 | 00.927 | 0.221 | 95.904 | 0.018 | Non-Inhibitor |
| 9 | 96.519 | 19.166 | 0.063 | 91.079 | 0.025 | Non-Inhibitor |
| 10 | 95.342 | 01.888 | 0.093 | 92.446 | 0.015 | Non-Inhibitor |
| 11 | 97.236 | 14.894 | 0.083 | 92.994 | 0.028 | Inhibitor |
| 12 | 96.392 | 10.333 | 0.072 | 97.118 | 0.018 | Inhibitor |
| 13 | 96.393 | 10.701 | 0.055 | 96.084 | 0.020 | Inhibitor |
| 14 | 96.607 | 04.677 | 0.051 | 95.323 | 0.026 | Inhibitor |
| 15 | 96.881 | 01.616 | 0.019 | 91.527 | 0.028 | Inhibitor |
| 16 | 97.556 | 02.949 | 0.019 | 89.257 | 0.058 | Inhibitor |
| 17 | 96.870 | 19.900 | 0.044 | 90.933 | 0.392 | Inhibitor |
| 18 | 96.658 | 13.684 | 0.077 | 97.741 | 0.019 | Inhibitor |
| 19 | 94.977 | 01.342 | 0.085 | 95.623 | 0.026 | Non-Inhibitor |
| 20 | 96.573 | 19.579 | 0.052 | 93.923 | 0.032 | Inhibitor |
| 21 | 95.317 | 02.807 | 0.059 | 94.393 | 0.019 | Non-Inhibitor |
| 22 | 97.118 | 16.052 | 0.057 | 95.841 | 0.025 | Inhibitor |

**Table 4:** Assessment of risk factors of substituted benzopyran-2-one derivatives using OSIRIS property explorer.

| Comp. | Mutagenic | Tumorigenic | Reproductive effective | Irritant |
|---|---|---|---|---|
| 1 | None | None | Low | None |
| 2 | None | None | None | None |
| 3 | None | None | None | None |
| 4 | High | None | None | None |
| 5 | None | None | High | None |
| 6 | None | None | None | High |
| 7 | None | None | High | None |
| 8 | None | None | None | None |
| 9 | None | None | None | None |
| 10 | None | None | None | None |
| 11 | None | None | High | None |
| 12 | None | None | Low | None |
| 13 | None | None | None | None |
| 14 | None | None | None | None |
| 15 | High | None | None | None |
| 16 | None | None | High | None |
| 17 | None | None | None | High |
| 18 | None | None | High | None |
| 19 | None | None | None | None |
| 20 | None | None | None | None |
| 21 | None | None | None | None |
| 22 | None | None | High | None |

## CONCLUSION

The molecular docking and *in silico* ADMET analysis of a series of substituted benzopyran-2-one derivatives was performed. The results revealed that active compounds bound in target site of α-glucosidase very effectively with most active compounds exhibiting multiple interactions like hydrogen bonding, hydrophobic and electrostatic interactions and as many as three hydrogen bonds were formed between active target site and ligand (7-hydroxy-6-methoxy-3-[4-(4-methyl-phenylsulfonamido) benzoyl]-2H-1-benzopyran-2-one). Some other interactions like pi-pi T shaped, pi-pi stacking and pi-anion interactions were also observed. The role of hydroxyl group and sulphamoyl group was also unleashed as it displayed strong interactions with enzyme active site. The *in silico* ADMET analysis also favored the activity of these compounds. The study will help researchers working on anti-diabetic molecules to consider similar types of compounds, particularly hydroxyl substitution and sulfamoyl group, to be considered as lead molecules for the development of effective anti-diabetic molecules.

**ACKNOWLEDGEMENTS**

The authors gratefully acknowledge Dr. A. P. J. Abdul Kalam Central Instrumentation laboratory, G. J. U. S. and T., Hisar for Junior Research Fellow (JRF) award to Ms. Samridhi Thakral under DST-PURSE programme. The authors are also thankful to Chairman, Department of Pharmaceutical Sciences, Guru Jambheshwar University of Science and Technology, Hisar for providing necessary facility for this work.

**REFERENCES**

[1] Popovic-Djordjevic, J.B., et al. Stanojković, α-glucosidase inhibitory activity and cytotoxic effects of some cyclic urea and carbamate derivatives. *J. Enzyme Inhib. Med. Chem*., **2017.** 32(1): 298-303.

[2] Shahidpour, S.M., et al., Synthesis of novel poly-hydroxyl functionalized acridine derivatives as inhibitors of α-glucosidase and α-amylase. *Med. Chem. Res*, **2015.** 24(7): 3086-3096.

[3] Gupta, S.J., et al., Synthesis, *in vitro* evaluation and molecular docking studies of novel amide linked triazolyl glycoconjugates as new inhibitors of α-glucosidase. *Bioorg. Chem*, **2017.** 72: 11-20

[4] Luthra, T., et al., A novel library of -arylketones as potential inhibitors of α-glucosidase: Their design, synthesis, *in vitro* and *in vivo* studies. *Sci. Rep*, **2017.** 7(1): 13246.

[5] Ferreira, LG., et al., Molecular docking and structure-based drug design strategies. *Molecules*, **2015.** 20(7): 13384-13421.

[6] Haque, R., et al. Use of Crowd-funding for developing social enterprises: An Islamic approach. *Mod. Appro. Drug Des*., **2018.** 1(4): MADD.000518

[7] Elokely, K.M., and Doerksen, R.J., Docking challenge: Protein sampling and molecular docking performance. J. Chem. Inf. Model., **2013.** 53(8): 1934-1945.

[8] Meng, X.Y., et al. Molecular docking: A powerful approach for structure-based drug discovery. Curr. *Comput. Aided Drug Des*., **2011.** 7(2): 146-157.

[9] Singh, R., et al. *Lett. Drug Des. Discov*., **2017**. 14(5): 540-553.

[10] Judge, V., et al. Synthesis, anti-microbial, anticancer, antiviral evaluation and QSAR studies of 4-(1-aryl-2-oxo-1,2-dihydro-indol-3- ylideneamino)-N-substituted benzene sulfonamides. *Med. Chem.,* **2013.** 9(1): 53-76.

[11] Judge, V., et al. Synthesis, *in vitro* antimicrobial, antiproliferative, and QSAR studies of N-(substituted phenyl)-2/4-(1H-indol-3-ylazo)-benzamides. *Med. Chem. Res,* **2011.** 21(7): 1-13.

[12] Wang, S., et al., Salicylic acid based small molecule inhibitor for the oncogenic Src Homology-2 domain containing protein tyrosine phosphatase-2 (SHP2). *Eur. J. Med. Chem***., 2010**. 45: 1250-1255.

[13] Rahim, F., et al. Isatin based Schiff bases as inhibitors of α-glucosidase: Synthesis, characterization, *in vitro* evaluation and molecular docking studies. *Bioorg. Chem***., 2015.** 60: 42-48.

[14] Biasini, M., et al., SWISS-Model: Modelling protein tertiary and quaternary structure using evolutionary information. *Nucleic Acids Res*., **2014.** 42(W1): W252-W258.

[15] Yamamoto, K., et al. Crystal structures of isomaltase from *Saccharomyces cerevisiae* and in complex with its competitive inhibitor maltose. *FEBS J.,* **2010**. 277(20): 4205-4214.

[16] Berendsen, HJC., et al. The missing term in effective pair potentials. *J. Phys. Chem*., **1987.** 91(24): 6269-6271.

[17] Jorgensen, W.L., and Tirado-Rives, J., The OPLS [Optimized Potentials for Liquid Simulations] potential functions for proteins, energy minimizations for crystals of cyclic peptides and crambin. *J. Am. Chem. Soc*., **1988.** 110(6): 1657-1666.

[18] Van Der Spoel, D., and Lindahlet, E., GROMACS: fast, flexible, and free. *J. Comput. Chem.,* **2005.** 26(16): 1701-1718.

[19] Trott, O., and Olson, J.A., AutoDock Vina: Improving the speed and accuracy of docking with a new scoring function, efficient optimization, and multithreading. *J. Comput. Chem*., **2010.** 31: 455-461.

[20] Dassault Systèmes BIOVIA, Discovery studio visualizer. v16.1.0.15350, San Diego: *Dassault Systèmes*, **2016.**

[21] El-Gohary, NS., and Shaaban, MI., Antimicrobial and antiquorum-sensing studies. Part 3: Synthesis and biological evaluation of new series of [1,3,4] thiadiazoles and fused [1,3,4] thiadiazoles. *Arch. Pharm*., **2015.** 348(4): 283-297.

[22] Murugavel, S., Experimental and computational approaches of a novel methyl (2E)-2-{[N-(2-formylphenyl) (4-methylbenzene) sulfonamido] methyl}-3-(4-chlorophenyl) prop-2-enoate: A potential antimicrobial agent and an inhibition of penicillin-binding protein. *J. Mol. Struct.*, **2016.** 1115: 33-54.

[23] K.N. de Oliveira, M.M. Souza, P.C. Sathler et al., Sulphonamide and sulphonyl-hydrazone cyclic imide derivatives: antinociceptive activity, molecular modeling and *in silico* ADMET screening. *Arch. Pharm. Res*.**, 2012**, 35(10), 1713-1722.

[24] Lipinski, C.A., et al. Experimental and computational approaches to estimate solubility and permeability in drug discovery and development settings. *Adv. Drug Deliv. Rev*.**, 2001.** 46(1-3): 3-26.

[25] Veber, D.F., et al., Molecular properties that influence the oral bioavailability of drug candidates. *J. Med. Chem.*, **2002.** 45(12): 2615-2623.

[26] T.S Patel, et al. Novel 2,3-disubstituted quinazoline-4(3H)-one molecules derived from amino acid linked sulphonamide as a potent malarial antifolates for DHFR inhibition. Dixit, Eur. *J. Med. Chem.*, **2017.** 129: 251-265.

[27] Balam, SK., et al., Synthesis of N-(3-picolyl)-based 1,3,2λ5-benzoxazaphosphinamides as potential 11β-HSD1 enzyme inhibitors. *Med. Chem. Res***, 2015.** 24(3): 1119-1135.